Review paper: The 10th March 1970 Mw 5.0 Calingiri surface rupturing earthquake, Australia

Tamarah King

    School of Earth Sciences, The University of Melbourne, Victoria 3010, Australia
    tamarah.king@unimelb.edu.au
    https://orcid.org/0000-0002-9654-2917

Mark Quigley

    School of Earth Sciences, The University of Melbourne, Victoria 3010, Australia
    Mark.quigley@unimelb.edu.au
    https://orcid.org/0000-0002-4430-4212

Dan Clark

    Geoscience Australia, Canberra 2601, Australia
    https://orcid.org/0000-0001-5387-4404

Abstract

The 10th March 1970 moment magnitude (M_W) 5.0 Calingiri earthquake surface rupture is 3.3 km long with a maximum vertical displacement of 0.4 m. The fault as defined by surface measurements is a shallow-dipping reverse fault (~ 20° east) with a probable shallow hypocentre (< 1 km). This is consistent with published hypocentral depths, though large uncertainties exist within the seismological data. The finest-resolution geological map available for the epicentral area (1:250 000) indicates the presence of granitic gneiss and migmatite outcrops within a few kilometres of the surface rupture with foliations striking sub-parallel to the surface rupture trace but with near-vertical dips. The rupture is subparallel to linear geophysical anomalies suggesting a bedrock structural control to faulting. There is no evidence to suggest prior Pleistocene surface rupture along the Calingiri scarp, although no detailed palaeoseismic investigations have been conducted.

This document presents a review of available literature related to the 1970 Calingiri surface rupturing earthquake. It includes newly digitised data related to the rupture and new interpretations of controls on fault rupture. It supplements a manuscript reviewing all Australian surface rupturing earthquakes, submitted to Geosciences in August 2019.

Please contact authors on the content presented herein; we welcome constructive feedback.

1. Geology

1.1 Regional

The 1970 Mw 5.0 Calingiri earthquake is one of a series of historical surface rupturing earthquakes (1968 Meckering, 1970 Calingiri, 1979 Cadoux, 2008 Katanning, and 2018 Lake Muir) (Dawson et al., 2008; Gordon and Lewis, 1980; Lewis et al., 1981) hosted within the South-West Seismic Zone (SWSZ) in southern Western Australia (Doyle, 1971). The SWSZ resides predominately within the Yilgarn Craton (*Figure 1*), an assemblage of predominately Archean granitoid-greenstone rocks (Wilde et al., 1996).
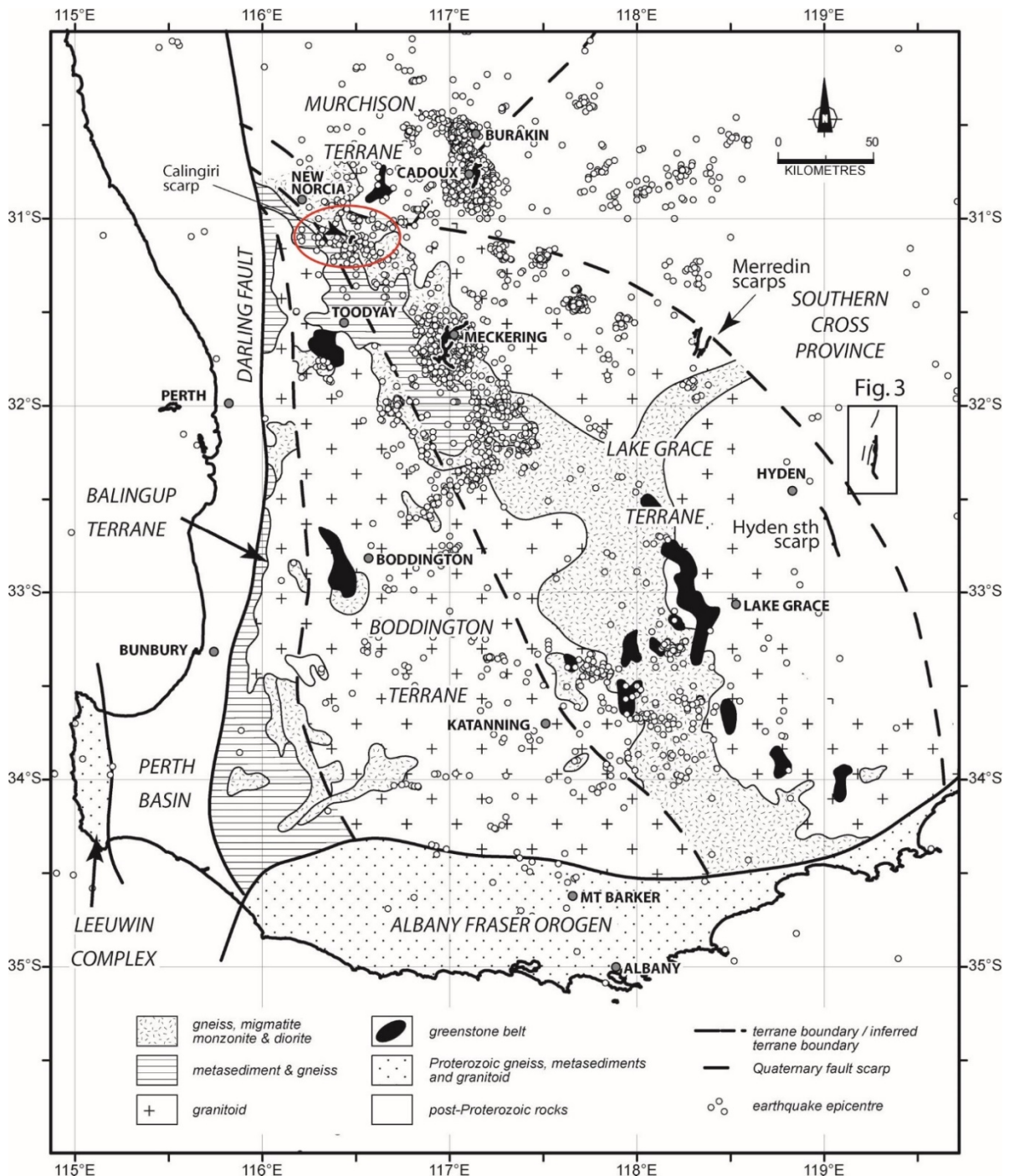

Figure 1: Regional geology surrounding the Calingiri earthquake and SWSZ. Figure2 from Clark et al. (2008)

44 The SWSZ extends roughly NW-SE within a region of the Yilgarn Craton consisting of poly-
45 deformed and metamorphosed crystalline basement (*Figure 1*). The SWSZ extends across three
46 tectono-stratigraphic terranes; the Boddington Terrane, Lake Grace Terrane and Murchison Terrane
47 (Dentith and Featherstone, 2003; Wilde et al., 1996). Due in part to few basement outcrops, the
48 boundaries between terranes are poorly constrained. Gravity data show that the boundary between the
49 Boddington and Lake Grace Terranes is a major east-dipping geological structure (Clark et al., 2008;
50 Dentith and Featherstone, 2003), interpreted as a large thrust zone based on dating and metamorphic
51 facies analysis across the two terranes (Wilde et al., 1996). Historic seismicity generally aligns with
52 this structure, and occurs on the eastern side of it (Dentith and Featherstone, 2003).

53 The Calingiri earthquake occurred in the northern area of the Jimperding Metamorphic Belt (*Figure
54 1*), within the Lake Grace Terrane, but close to the mapped boundaries with the Boddington and
55 Murchison Terranes. The Jimperding belt consists of "repeatedly deformed granitoids, gneisses, belts
56 of metasedimentary rocks, small greenstone belts and remnants of layered basic intrusions" (Dentith
57 and Featherstone, 2003).

1.2 Local bedrock

59 No bedrock outcrops were mapped near the Calingiri scarp by Gordon and Lewis (1980). They do
60 describe "vertically foliated Archean migmatites and metasediments" to the west of Calingiri,
61 "equigranular granite" to the north-east of the town, and "a few" dolerite dykes and quartz veins. The
62 Western Australia Geological Survey 1:250,000 geological map (Wilde et al., 1978) (*Figure 3*) shows
63 basement outcrops of banded migmatite and granitic gneiss in the rupture area with the majority of
64 foliation trending towards the NE, coincident with strike of rupture. The dips of planar fabric elements
65 within these surface outcrops are near-vertical in most locations, whereas dips of the faults underlying
66 the rupture are ~ 20° (Section 3.2.3.). The surface rupture strikes subparallel to a magnetic anomaly,
67 and the edge of a minor gravitational anomaly *Figure 2*.

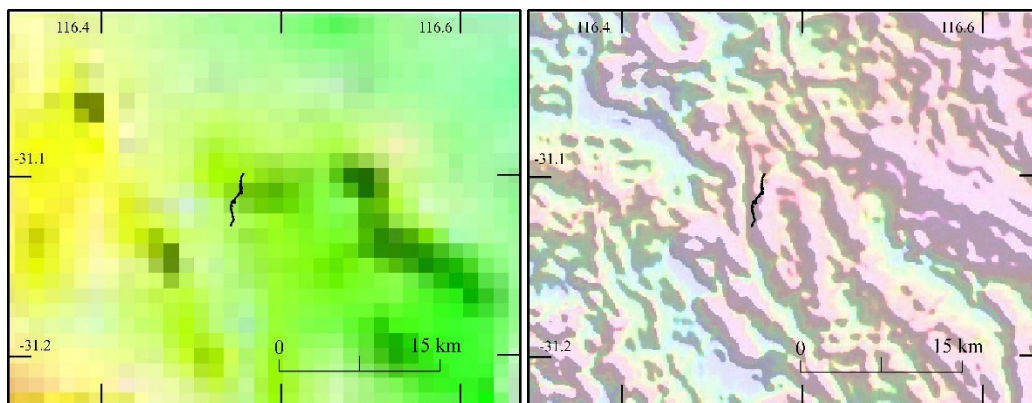*Figure 2: Calingiri scarp (black lines) relative to magnetic intensity and bouguer gravity anomaly maps. National bouguer gravity anomaly map: http://pid.geoscience.gov.au/dataset/ga/101104; National total magnetic intensity map: http://pid.geoscience.gov.au/dataset/ga/89596*

1.3 Surficial deposits

69 Authors investigating the event do not describe the local geology or surface sediments in detail. The
70 available 1:250,000 geological map of the area (Wilde et al., 1978) shows the rupture associated with
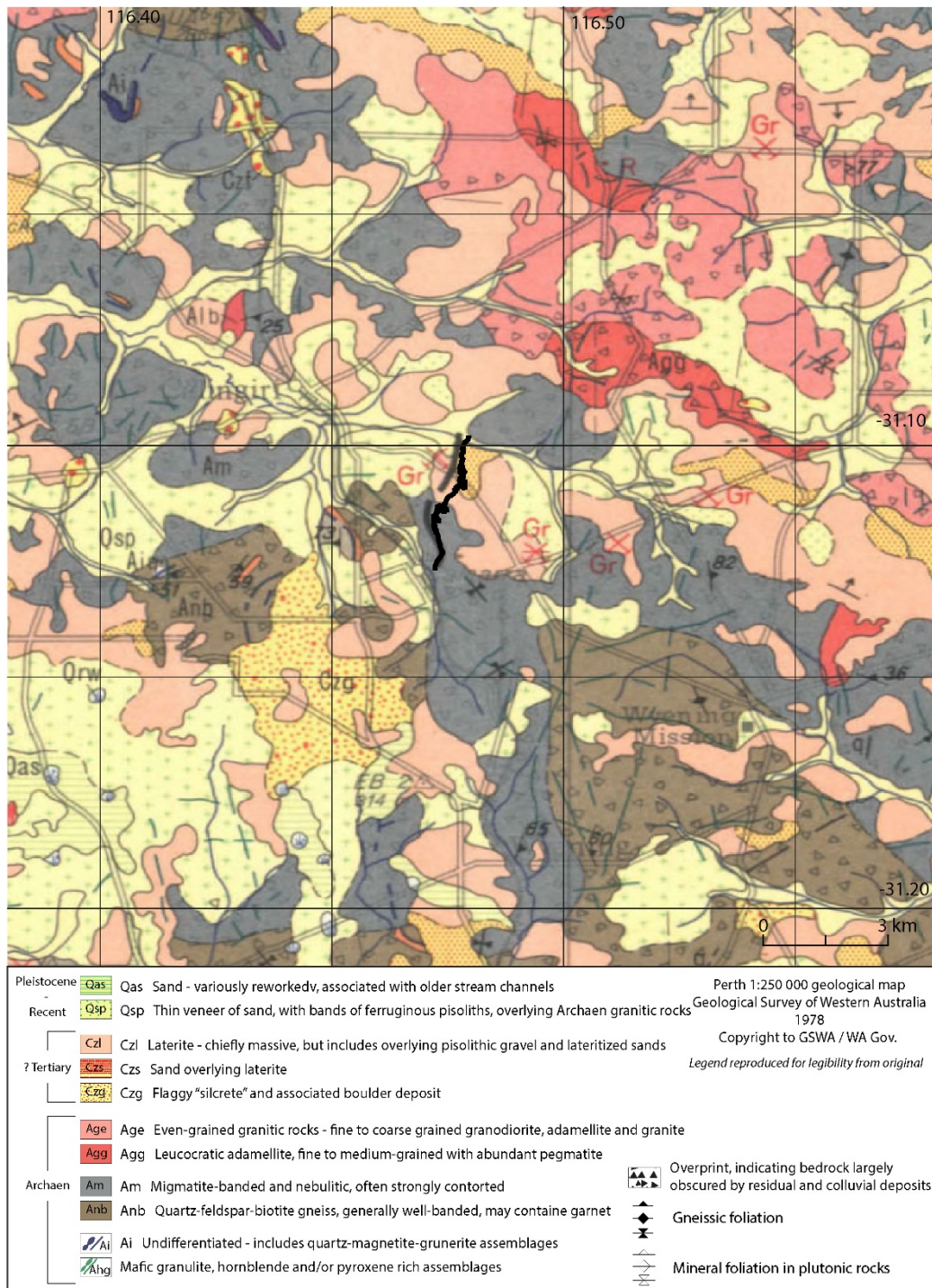71 "Cenozoic laterite" and "quartzose duricrust" (*Figure 3*).

Figure 3: Crop of Perth 1:250 000 geological map sheet (Wilde et al., 1978) showing basement and surface sediments around the Calingiri surface rupture. Full map and legend available from: http://www.dmp.wa.gov.au/Geological-Survey/GSWA-publications-and-maps-1399.aspx

2. Seismology

2.1 Epicentre and magnitude estimates

No relocation of the epicentre has taken place, with the current Geoscience Australia (GA) online catalogue location the same coordinates as the original reported location (Gregson, 1971) (Table 1). The location is on the footwall 700 m from the surface rupture though uncertainty may be in the order of ± 1 – 10 km, so the true epicentre is likely on the hanging-wall of the surface rupture (*Figure 4*). The GA NSHA18 catalogue (Allen et al., 2018) epicentre is located ~5 km NE of the other epicentres,

79   it is not known how this was derived (*Figure 4*). No uncertainties are published regarding the
80   Calingiri epicentre location in the original reports on the event.

81   This paper prefers the magnitude (M_W) of the recently published NSHA18 catalogue (Allen et al.,
82   2018) as they conduct a thorough and consistent reanalysis of Australian magnitude values,
83   particularly to address inconsistencies in the determination of historic magnitude values. Prior to this
84   reanalysis, the magnitude of the Calingiri earthquake was reported as 5.7 – 6.2 using various local
85   magnitude formula (M_L). These almost one magnitude unit higher than the revised NSHA18
86   magnitude, which has implications for any previous scaling relationships incorporating older
87   magnitudes.

88   *Table 1 : Published epicentre locations, depths and magnitudes*

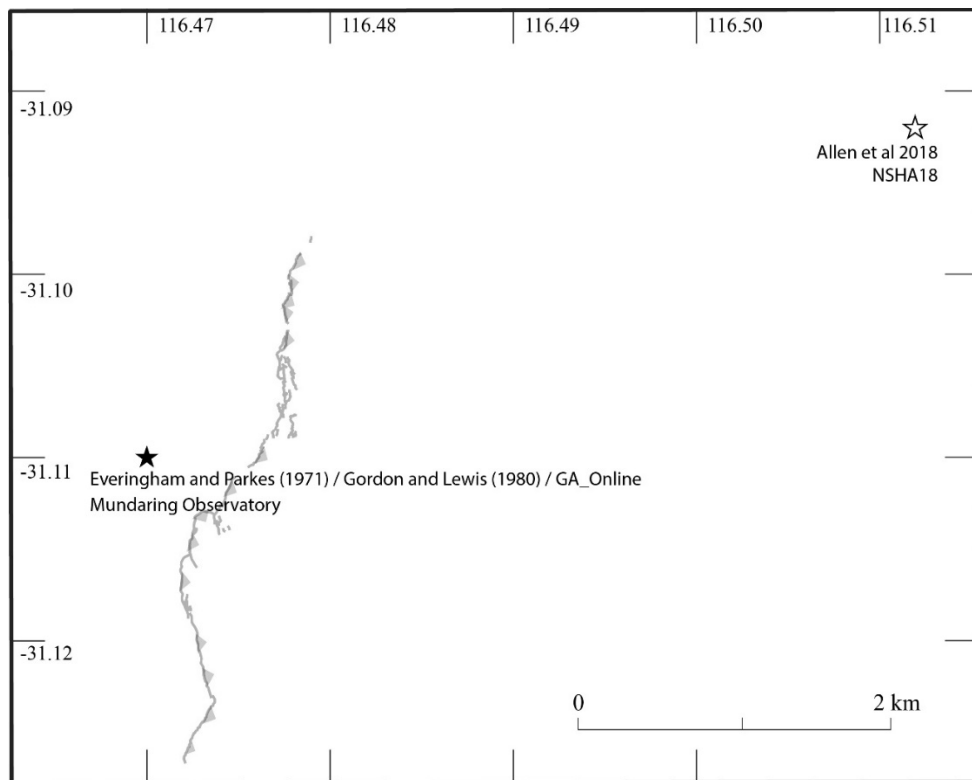| Reference	Agency	Latitude	± (km)	Longitude	± (km)	Depth	± (km)	M1		M2		M3	
GA_online	GA	-31.11		116.47		1		5.7	Mw	5.9	ML	5.5	mb
Everingham and Parkes (1971)	Mundaring Observatory	-31.11		116.47		1		5.7	M	6.2	M	5.1	MS
Gordon and Lewis (1980)	Mundaring Observatory	-31.11		116.47		1		6.2	ML	5.7	M		
Allen et al (2018)	NSHA18	-31.092		116.512		15		5.03	Mw	5.9	ML		

89

Figure 4: Published epicentre locations around the surface rupture

90   **2.2 Focal mechanisms**

91   Fitch et al. (1973) published the only focal mechanism for the Calingiri rupture, a lower hemisphere
92   solution which shows a reverse mechanism with a dextral component to movement along a preferred
93   plane trending 056° and dipping 50° to the east (based on surface rupture) (*Figure 5*). Gordon and

94   Lewis (1980) report sinistral movement on a fault striking 337° and dipping 76°E based on the Fitch
95   et al. (1973) solution, however this plane of the focal mechanism actually describes a sinistral west
96   dipping fault. As noted by Leonard et al. (2002), the Fitch et al. (1973) solution is based on short
97   period instrument recordings, has uncertainties of 120 – 100° and was constrained by their solution for
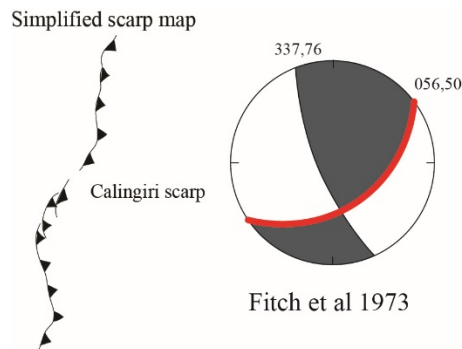98   the Meckering earthquake.

Figure 5: Published focal mechanism, preferred rupture plane from the publication highlighted in red.

99   **2.3 Depth**

100   Gregson (1971) report a depth of 1 km derived by the USGS, also the depth used in Everingham and
101   Parkes (1971) and Gordon and Lewis (1980). Fitch et al. (1973) report a depth of 15 km in their focal
102   mechanism solution, too deep to have produced a surface rupture.

103   **2.1 Foreshock / aftershocks**

104   The Calingiri area experienced three (assumed to be M_L) > 4.0 earthquakes prior to the 1968
105   Meckering earthquake, which triggered increased seismicity in the region. In 1952 an earthquake (of
106   unspecified magnitude) is reported to have caused structural damage to a new school building, with an
107   epicentral location determined 13 km north of the township (Gordon and Lewis, 1980). In 1955 the
108   Mundaring Observatory reported a magnitude 4.7 earthquake approximately 19 km north of the town,
109   while in 1963 a magnitude 4.9 event was located 13 km north (Gordon and Lewis, 1980). Calingiri
110   experienced seventeen events between M_L 2.6 - 4.4 from October 1968 (the Meckering earthquake) to
111   November 1969 (the Calingiri mainshock occurred 4 months later) (Everingham and Gregson, 1971;
112   Gordon and Lewis, 1980; Gregson, 1971).

113   One temporary seismometer was deployed by Mundaring Observatory, but the instrument failed and
114   recorded no earthquakes (Gregson, 1971). Following the Calingiri mainshock only nine aftershocks
115   are recorded in the area, with magnitudes ranging from M_L 3.0 - 4.0. The Mundaring Observatory
116   reports foreshocks down to magnitude M_L 2.6, so we consider this to represent the catalogue
117   completeness value for this area at this time. Therefore, the Calingiri event shows a lack of immediate
118   aftershock activity, with a M_L 3.8 recorded in July (4 months after the mainshock), 3.1 in October (7
119   months) and the largest aftershock with M_L 4.0 occurring in December 1970 (9 months). No events >
120   M_L 2.6 were recorded in the area from 1973 - 1980. Given this aftershock temporal distribution,
121   Gordon and Lewis (1980) consider the Calingiri mainshock as an aftershock to the larger Meckering
122   event, though this is not consistent with current methods for determining maximum distances of
123   aftershocks (e.g. those used in Allen et al. (2018)).

124   **3. Surface Rupture**

125   **3.1 Authors / map quality**

126   The Calingiri rupture is located on a pastoral property 152 km drive north of Perth. The first
127   descriptions of the Calingiri surface rupture come from seismological reports from the Mundaring
128   Geophysical observatory, located 120 km south of the rupture (Everingham and Gregson, 1971;

129 Gregson, 1971). The only published detailed mapping of the rupture is a 1:10,000 map in Gordon and
130 Lewis (1980) with mapping conducted 1 - 2 months after the rupture. The rupture trace from this map
131 is reproduced in the GA Neotectonics Features database (Clark, 2012). Gordon and Lewis (1980) note
132 that farming had removed surficial evidence of rupture, though some sections of are still visible in
133 Google and Bing satellite imagery. The rupture trace from the GA Neotectonics Features and sections
134 visible in Google and Bing satellite imagery do not align (e.g. -31.12, 116.47) due to datum
135 transformation issues and simplification of fine-scale morphology in the original map.
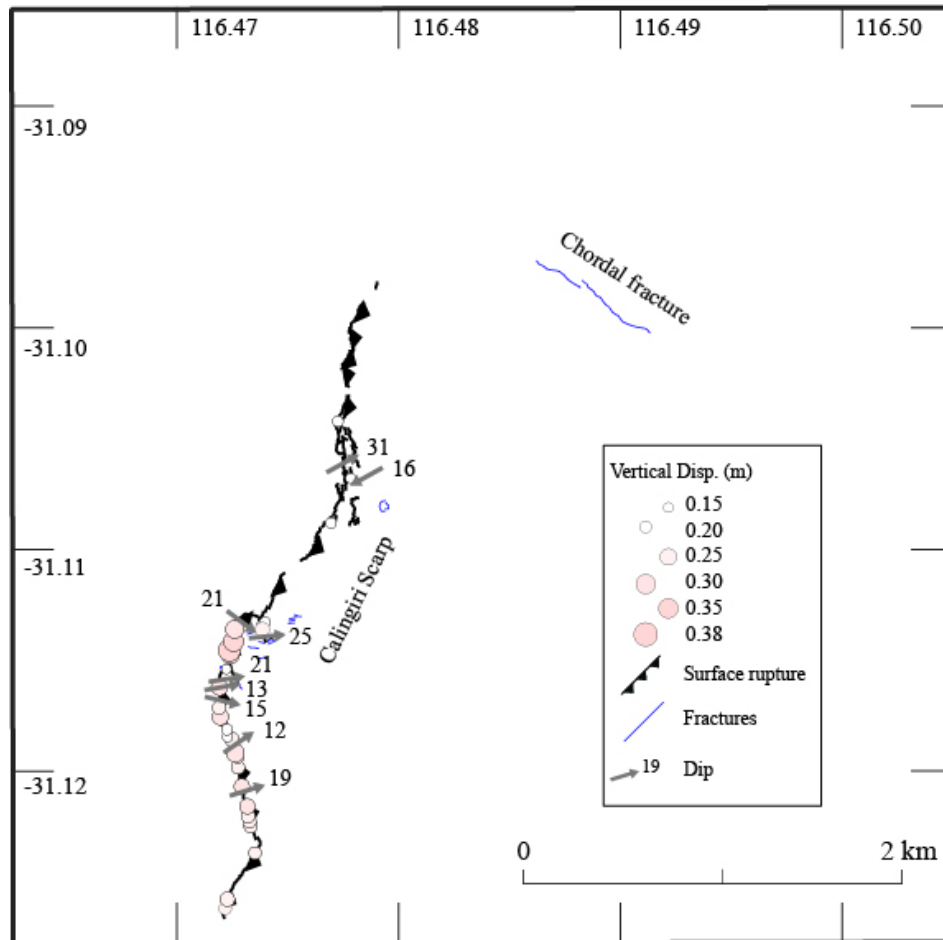

Figure 6: *Map of the Calingiri scarp, fractures, vertical offset measurements, and dip measurements (data digitised from* Gordon and Lewis (1980))

136   **3.2 Length and shape**

137 Initial reports describe a 5 km long rupture (Everingham and Gregson, 1971; Gregson, 1971),
138 however Gordon and Lewis (1980) describe 3.3 km long scarp, and this is the length reported in
139 subsequent publications (Figure 7b). This length results from measuring the rupture from north to
140 south along a straight line. Applying a criteria which simplifies ruptures to straight traces and defines
141 distinct faults where mapped primary rupture has gaps/steps > 1 km and/or where strike changes by >
142 20° for distances > 1 km (e.g. (Quigley et al., 2017)) results in the same length (explored in more
143 detail in King et al. (2019) (in review)). The length of the causative fault, assuming a relatively
144 straight plane, is likely to be slightly longer than the simplified 3.3 km long trace, as the fault will not
145 have ruptured to the surface along its full length.

146 Figure 7c maps portions of the scarp where more than two vertical displacement measurements of
147 greater than 0.2 m occur within a distance of 1 km (data from Gordon and Lewis (1980)). Given
148 granitic basement cosmogenic erosion rates in equivalent arid settings of Australia of 0.3 – 5 m/Myr
149 (Bierman and Caffee, 2002), 0.2 m of scarp height would be removed within 35 – 660 kyrs, leaving

150   ~1 km of rupture still visible in the landscape. This indicates that the feature is unlikely to be
151   persistent in the landscape over the time frame typical of the recurrence interval observed on nearby
152   faults in the SWSZ (e.g. Hyden, Dumbleyung (Clark et al., 2008; Estrada et al., 2006)). In this
153   calculation we do not account for erosion rates of any duricrust which may overlie granitic bedrock,
154   for differential erosion rates across the rupture topography, or increased erosion from past climatic
155   changes or modern processes.

156   The mapped surface rupture trace by Gordon and Lewis (1980) shows discontinuous segments of 50 –
157   500 m in length with breaks up to 150 m (*Figure 6*, *Figure 7*). It has an overall shape that is slightly
158   concave, with concavity defined by short (< 500m) oblique linear segments. Longer Australia surface
159   ruptures (e.g. Meckering, Cadoux) have similar deviations of strike orientation across short distances
160   (e.g. < 500 m).

161   A 600 m long secondary scarp (the 'Calingiri Chordal Fault') is mapped on the hanging-wall ~1 km
162   away from the northern tip of the main rupture (*Figure 6*, Figure 7). Gordon and Lewis (1980) report
163   that the property owner observed this scarp six weeks following the main rupture and stated that it had
164   not been visible on multiple previous visits to the field. This scarp is mapped as a series of en echelon
165   extensional fractures and may better be described as secondary extensional fractures related to
166   hanging-wall relaxation rather than a primary rupture, although its possible genesis from an
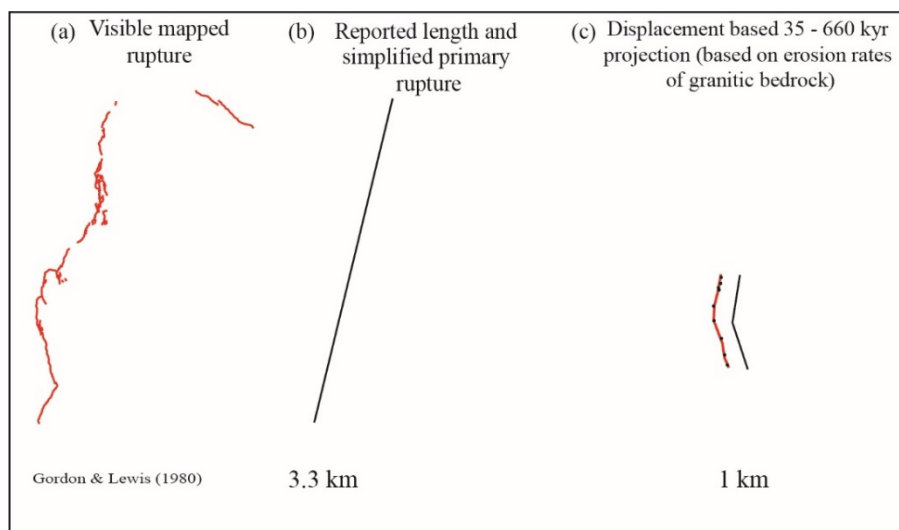167   aftershock cannot be dismissed.

Figure 7: Various measures of length for the Calingiri rupture and underlying fault as described in the text.

3.3 Strike

169   The rupture trends towards 011° on average, with deviations along its length describing trends
170   between 346 – 030°. The secondary extensional fracture ('chordal fault') trends toward 306°.

3.4 Dip

172   Gordon and Lewis (1980) show dip measurements along the rupture ranging from 12 - 31° on their
173   map of the rupture (Figure 6), with an average of 19°. The report mentions shallower dips of 10°
174   measured where the rupture crosses a stream and drain. They relate dip variations to surficial
175   sediment competency. They calculate an overall dip of 40° east based on slip (horizontal and vertical
176   components of displacement).

177   The only reported seismologically derived dip comes from Fitch et al. (1973) who find a 50° dip on
178   the east dipping plane (*Figure 5*). As previously described, Gordon and Lewis (1980) identify the
179   incorrect plane of the Fitch et al. (1973) solution and describe the dip as 76° NE, which matches the

180 SW dipping plane. The Fitch et al. (1973) solution for dip has uncertainties as described for the focal
181 mechanism.

3.5 Morphology

183 The southern section of the Calingiri scarp generally shows a single discrete rupture with short step-
184 overs or ramp structures (Gordon and Lewis, 1980). The northern section is characterized by single
185 discrete ruptures or pressure ridges, often discontinuous over short distances, or with multiple
186 duplexing discrete ruptures. As with the Meckering scarp, Gordon and Lewis (1980) note that the
187 rupture morphology seemed related to surficial sediments, low compression ridges in sandy soil and
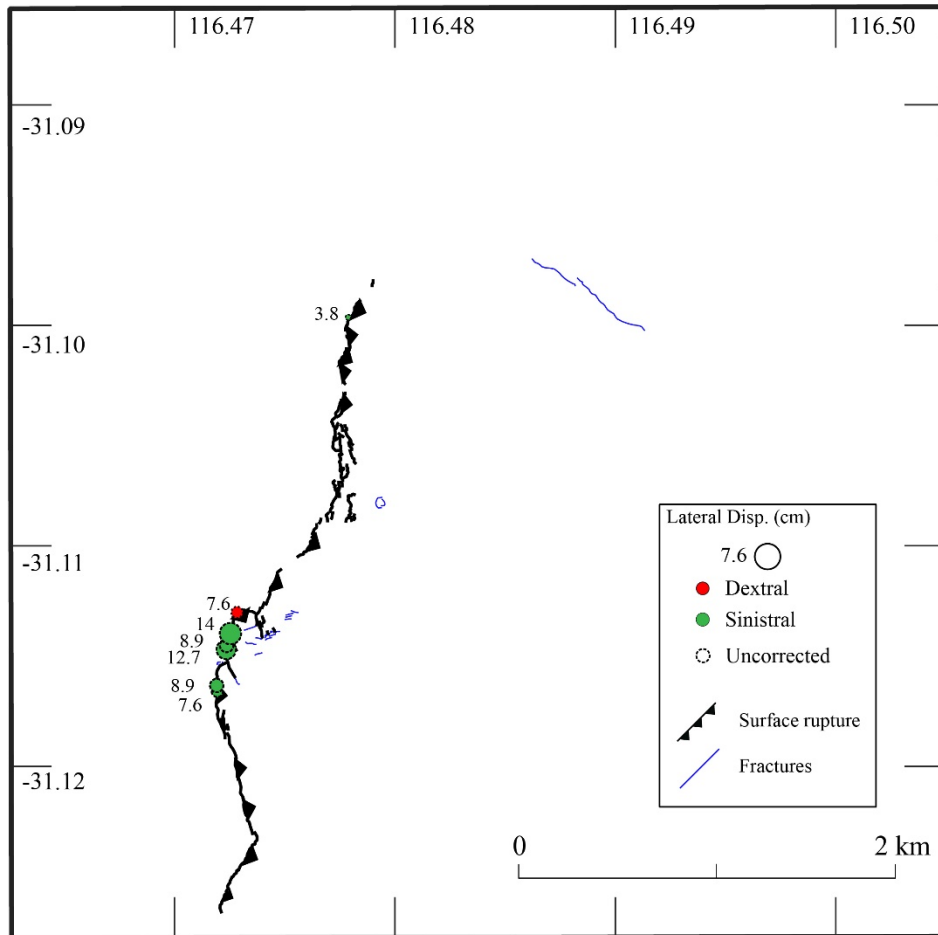188 larger discrete ruptures in lateritic soils.

Figure 8: Lateral displacement measurements (in cm) digitised from Gordon and Lewis (1980). Uncorrected measurements (all measurements) are offsets measured from features (fences, roads, etc) not perpendicular to the strike of surface rupture.

3.6 Kinematics

190 Gordon and Lewis (1980) describe the Calingiri fault as a sinistral thrust, recording predominately
191 sinistral movement where measurements were taken of offset features (Figure 8). All measurements
192 are uncorrected for the horizontal angle between the rupture and offset feature, so true lateral offset is
193 unknown (e.g. if not perpendicular, lateral offset may appear greater or less than true offset).
194 Stepovers and fractures in the central and southern sections of rupture support a sinistral
195 compressional step, though the breaks between segments in the northern section show a dextral
196 extensional sense of movement, and step overs in the northern segment could be either dextral
197 compression or sinistral extension.

3.7 Displacement

199 Vertical and lateral offset along the rupture is mapped in plate 6 of Gordon and Lewis (1980), but no
200 description exists for how these measurements were obtained, so we cannot estimate measurement
201 uncertainty. No levelling profiles were published for this rupture, and no surveying along the scarp is
202 described in published sources. The digitised data (methods in Appendix A) show an asymmetrical
203 along-rupture displacement envelope concentrated on the southern scarp, with maximum offset in the
204 central most arcuate section of rupture (Figure 9). Only three offset measurements are recorded along
205 the northern section of scarp, though the text describes offsets of 7 – 8 cm along the majority of the
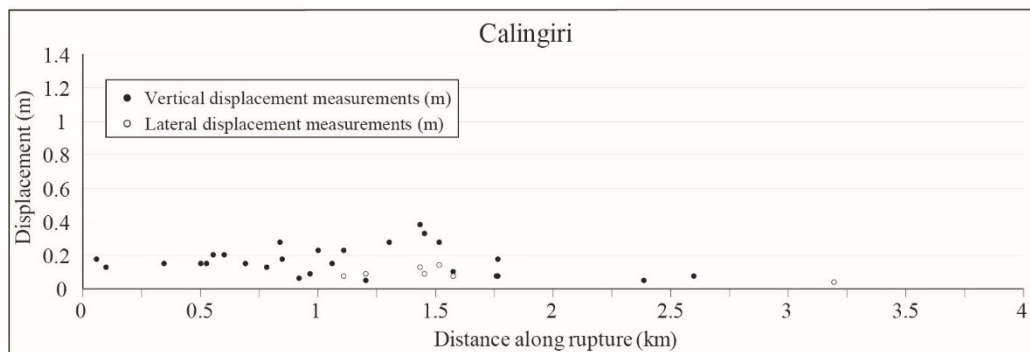206 scarp.

*Figure 9: Vertical and lateral displacement measurements along the Calingiri scarps, digitised
from (Gordon and Lewis, 1980). Methods described in Appendix A*

207 ### 3.8 Environmental damage

208 Based on length and maximum offset, the Calingiri surface rupture fits an ESI-07 scale measure of
209 IX, while fractures/cracking as described by Gordon and Lewis (1980) fits ESI V-VI (Michetti et al.,
210 2007). No other environmental damage is specifically documented that falls within the ESI-07 scale.
211 Gordon and Lewis (1980) note a single location where circular extensional cracking surrounded a
212 small tree, similar to descriptions of the Meckering rupture (Gordon and Lewis, 1980) and Petermann
213 rupture (King et al., 2018). Gordon and Lewis (1980) describe cracking identified near the Calingiri
214 rupture that appeared infilled and many years old, they suggest this may relate to the 1968 Meckering
215 earthquake based on the observed infill and level of degradation.

216 ## 4. Paleoseismology

217 No palaeoseismic investigations of the Calingiri rupture have been published. Gordon and Lewis
218 (1980) report scattered quartz fragments and thicker soil horizons in holes dug on the footwall
219 compared to several "missing" soil horizons on the hanging-wall, which they interpreted as supportive
220 evidence for past movement along a pre-existing fault. This evidence is circumstantial and could be
221 explained by several processes including differential weathering across lithological contacts or faults,
222 or a soil catena along the low relief hillslope which is coincident with the historic rupture.

223 ### 4.1 Slip rate

224 There is no evidence geological or geomorphic evidence to support prior rupture along the Calingiri
225 fault. The rupture is either the first neotectonic event, or the recurrence interval is sufficiently long
226 that all relief relating to prior event(s) was eroded prior to 1979 (e.g. 35 – 660 kyrs as discussed in
227 Section 3.2.1). If recurrence is assumed, vertical relief generation rates are limited by very low
228 bedrock erosion rates of < 5 m/Myr (Belton et al., 2004; Bierman and Caffee, 2002).

229 ## 5. Summary

230 ### 5.1 Relationship to Geology

231 The Western Australian Geological Survey 1:250,000 map (Wilde et al., 1978) shows migmatite and
232 gneissic basement in the rupture area, with foliation measurements varying between 140°/90°,
233 060°/90°, 180°/73° and 030°/59°. While variable, these measurements show some similarity to
234 surface rupture segments striking between 340 – 030°. The total magnetic intensity map shows a
235 potentially folded structure striking NW at the rupture location (Figure 2), consistent with strongly
236 deformed metasediments within the Jimperding Metamorphic Belt, including along the 1968
237 Meckering rupture (Dentith et al., 2009). The rupture generally strikes in the same direction as the
238 western limb of this structure.

5.2 Relationship to Seismology

240 The only focal mechanism for the Calingiri earthquake (Fitch et al., 1973) shows a dextral component
241 of slip on the east dipping plane with a strike of 056° which is oriented 20 - 40° clockwise relative to
242 the trend of the surface rupture. Gordon and Lewis (1980) misinterpret the focal mechanism
243 suggesting sinistral movement on a fault striking 337°. The surface rupture step-overs and gaps show
244 both dextral and sinistral senses of movement. Gordon and Lewis (1980) present predominately
245 sinistral measurements, with some dextral offset also recorded (Figure 8, Figure 9). Uncertainties
246 exist on the accuracy of the focal mechanism (see Section 2.2), and lateral offset measurements are
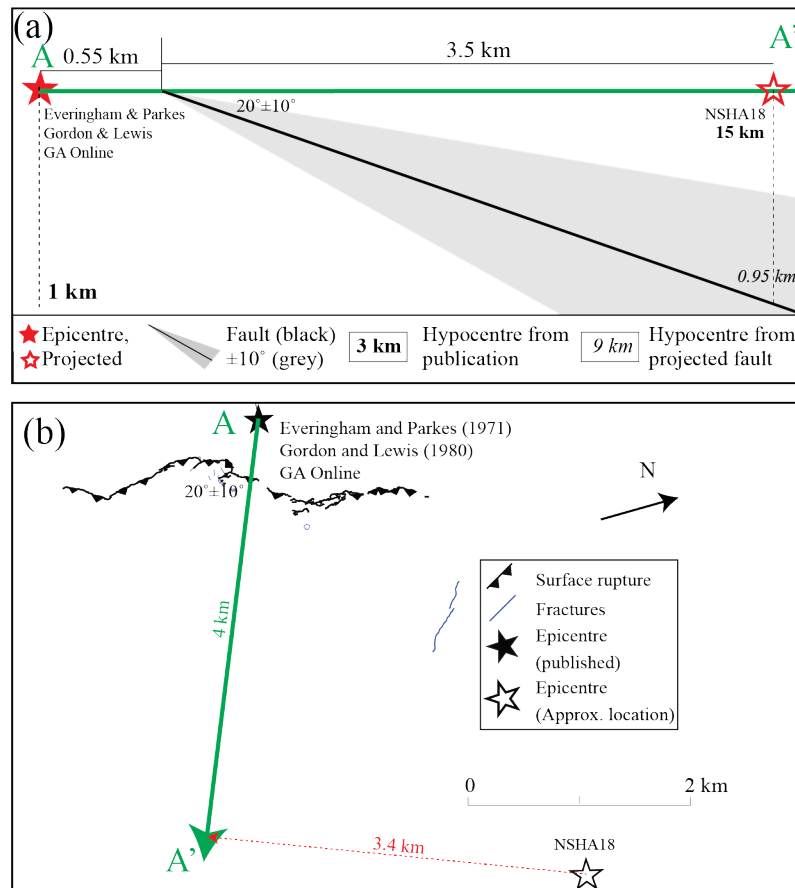247 uncorrected and therefore may be inaccurate.

Figure 10:Cross section across the Calingiri rupture showing epicentre locations as projected onto the cross section, depth of epicentres as published (bold) and depth to projected fault plane (italics) from surface dip data (from Gordon and Lewis (1980))

248 A cross section using measured dips from Gordon and Lewis (1980) shows how published epicentres
249 relate to the rupture at depth (Figure 10). The NSHA18 epicentre projects to approximately 1 km
250 depth based on simplified fault geometry. The uncertainty bounds on the footwall epicentre may be up
251 to 10km which could place it on the hanging-wall fault plane with potential depths 0 – 3.5 km (on a

252 20° dipping fault). Using the 40° preferred dip from Gordon and Lewis (1980) gives a depth range of
253 0 – 8 km. This is in line with other historic surface rupturing earthquakes where seismological
254 modelling shows centroid and hypocentral depths < 6 km (Fredrich et al., 1988; McCaffrey, 1989;
255 Vogfjord and Langston, 1987).

256

263

264   **6. References**

265 Allen, T., Leonard, M., Ghasemi, H., Gibson, G., 2018. The 2018 National Seismic Hazard
266   Assesment: Earthquake epicentre catalogue (GA Record 2018/30). Geoscience Australia,
267   Commonwealth of Australia, Canberra, ACT.
268   https://doi.org/http://dx.doi.org/10.11636/Record.2018.030

269 Belton, D.X., Brown, R.W., Kohn, B.P., Fink, D., Farley, K.A., 2004. Quantitative resolution of the
270   debate over antiquity of the central Australian landscape: Implications for the tectonic and
271   geomorphic stability of cratonic interiors. Earth Planet. Sci. Lett. 219, 21–34.
272   https://doi.org/10.1016/S0012-821X(03)00705-2

273 Bierman, P.R., Caffee, M.W., 2002. Cosmogenic exposure and erosion history of Australian bedrock
274   landforms. Bull. Geol. Soc. Am. 114, 787–803. https://doi.org/10.1130/0016-
275   7606(2002)114<0787:CEAEHO>2.0.CO;2

276 Clark, D., 2012. Neotectonic Features Database. Geoscience Australia, Commonwealth of Australia,
277   Canberra, Australia.

278 Clark, D., Dentith, M., Wyrwoll, K.-H., Yanchou, L., Dent, V.F., Featherstone, W.E., 2008. The
279   Hyden fault scarp, Western Australia: paleoseismic evidence for repeated Quaternary
280   displacement in an intracratonic setting. Aust. J. Earth Sci. 55, 379–395.
281   https://doi.org/10.1080/08120090701769498

282 Dawson, J., Cummins, P.R., Tregoning, P., Leonard, M., 2008. Shallow intraplate earthquakes in
283   Western Australia observed by Interferometric Synthetic Aperture Radar. J. Geophys. Res. Solid
284   Earth 113, 1–19. https://doi.org/10.1029/2008JB005807

285 Dentith, M., Clark, D., Featherstone, W.E., 2009. Aeromagnetic mapping of Precambrian geological
286   structures that controlled the 1968 Meckering earthquake (Ms 6.8): Implications for intraplate
287   seismicity in Western Australia. Tectonophysics 475, 544–553.
288   https://doi.org/10.1016/j.tecto.2009.07.001

289 Dentith, M., Featherstone, W.E., 2003. Controls on intra-plate seismicity in southwestern Australia.
290   Tectonophysics 376, 167–184. https://doi.org/10.1016/j.tecto.2003.10.002

291 Doyle, H.A., 1971. Seismicity and structure in Australia. Bull. R. Soc. New Zeal. 9.

292 Estrada, B., Clark, D., Wyrwoll, K.-H., Dentith, M., 2006. Paleoseismic investigation of a recently
293   identified Quaternary fault in Western Australia: the Dumbleyung Fault. Proc. Aust. Earthq.
294   Eng. Soc. Canberra ACT, Novemb. 2006 189–194.

295 Everingham, I.B., Gregson, P.J., 1971. Mundaring Geophysical Observatory, Annual Report, 1968

296   (BMR Record 1971/12). Bureau of Mineral Resources, Geology and Geophysics, Canberra,
297   Australia. https://doi.org/http://pid.geoscience.gov.au/dataset/ga/12549

298   Everingham, I.B., Parkes, A., 1971. Intensity Data for Earthquakes at Landor (17 June 1969) and
299   Calingiri (10 March 1970) and their Relationship to Previous Western Australian Observations
300   (BMR Recrod 1971/80), 1971/80. ed. Bureau of Mineral Resources, Geology and Geophysics,
301   Canberra, Australia. https://doi.org/http://pid.geoscience.gov.au/dataset/ga/12617

302   Fitch, T.J., Worthington, M.H., Everingham, I.B., 1973. Mechanisms of Australian earthquakes and
303   contemporary stress in the Indian ocean plate. Earth Planet. Sci. Lett. 18, 345–356.
304   https://doi.org/10.1016/0012-821X(73)90075-7

305   Fredrich, J., Mccaffrey, R., Denham, D., 1988. Source parameters of seven large Australian
306   earthquakes determined by body waveform inversion. Geophys. J. 95, 1–13.
307   https://doi.org/https://doi.org/10.1111/j.1365-246X.1988.tb00446.x

308   Gordon, F.R., Lewis, J.D., 1980. The Meckering and Calingiri earthquakes October 1968 and March
309   1970, Geological Survey of Western Australia Bulletin. Perth.

310   Gregson, P.J., 1971. Mundaring Geophysical Observatory Annual Report, 1970 (BMR Record
311   1971/77). Bureau of Mineral Resources, Geology and Geophysics, Canberra, Australia.
312   https://doi.org/http://pid.geoscience.gov.au/dataset/ga/12614

313   King, T.R., Quigley, M.C., Clark, D., 2019. Surface-rupturing historical earthquakes in Australia and
314   their environmental effects: new insights from re-analyses of observational data. Geosciences.

315   King, T.R., Quigley, M.C., Clark, D., 2018. Earthquake environmental effects produced by the Mw
316   6.1, 20th May 2016 Petermann earthquake, Australia. Tectonophysics 747–748, 357–372.
317   https://doi.org/10.1016/j.tecto.2018.10.010

318   Leonard, M., Ripper, I.D., Yue, L., 2002. Australian earthquake fault plane solutions (GA Record
319   2002/019), 2002/19. ed. Canberra, ACT.
320   https://doi.org/http://pid.geoscience.gov.au/dataset/ga/37302

321   Lewis, J.D., Daetwyler, N.A., Bunting, J.A., Montcrieff, J.S., 1981. The Cadoux Earthqauke (GSWA
322   Report 11). Perth, Australia.

323   McCaffrey, R., 1989. Teleseismic investigation of the January 22, 1988 Tennant Creek, Australia,
324   earthquakes. Geophys. Res. Lett. 16, 413–416. https://doi.org/10.1029/GL016i005p00413

325   Michetti, A.M., Esposito, E., Guerrieri, L., Porfido, S., Serva, L., Tatevossian, R.E., Vittori, E.,
326   Audemard M., F.A., Azuma, T., Clague, J., Comerci, V., Gurpinar, A., McCalpin, J.P.,
327   Mohammadioun, B., Morner, N.A., Ota, Y., Roghozhin, E., 2007. Intensity Scale ESI 2007,
328   Memorie Descrittive della Carta Geologica d'Italia, Special Volume 74. APAT, Rome 2007.

329   Quigley, M.C., Mohammadi, H., Duffy, B.G., 2017. Multi-fault earthquakes with kinematic and
330   geometric rupture complexity : how common ? INQUA Focus Group Earthquake Geology and
331   Seismic Hazards.

332   Vogfjord, K.S., Langston, C.A., 1987. The Meckering earthquake of 14 October 1968: A possible
333   downward propagating rupture. Bull. Seismol. Soc. Am. 77, 1558–1578.

334   Wilde, S.A., Low, G.H., Lake, R.W., 1978. Perth 1:250 000 Geological Map Sheet. Geological
335   Survey of Western Australia, Perth, Western Australia.

336   Wilde, S.A., Middleton, M.F., Evans, B.J., 1996. Terrane accretion in the southwestern Yilgarn
337   Craton: evidence from a deep seismic crustal profile. Precambrian Res. 78, 179–196.
338   https://doi.org/10.1016/0301-9268(95)00077-1

339

340   **Appendix A**

341 **Methods for digitising vertical displacement data**

342 The only offset measurements published for the Calingiri scarp are mapped along the scarp in Plate 6
343 of Gordon and Lewis (1980). This map was georeferenced against satellite imagery based on the
344 locations of roads, fences, and train tracks. The locations and vertical offset were recorded into a new
345 point shapefile. A simplified rupture trace was created for the scarps, and a short script[1] was used in
346 QGIS attribute manager field calculator to extract the distance of each vertical offset measurement
347 along the simplified rupture trace. The shape file was extracted into a final CSV with x-y coordinates,
348 vertical offset measurements, and distance along rupture data.

349 Dip data were digitised into a point shape file from a georeferenced version of Plate 5 from Gordon
350 and Lewis (1980).

---

[1] line_locate_point(geometry:=geometry(get_feature('Line', 'id', '1')), point:=$geometry)